norepinephrine uptake into brain nerve endings such as those observed in the two models of fighting stress reported here. It is possible that when "normal" or "abnormal" changes in mood or mental function occur as sequelae to chronic psychosocial stress, one important underlying mechanism may be a sustained alteration of the normal neuronal uptake of norepinephrine in the brain (*11*).

Note added in proof: After this report was submitted for publication, we found that the K_m for norepinephrine uptake in the cerebral cortex was increased immediately (68 percent, $P < .05$) after a single fighting episode in previously isolated mice, with no alterations in V_{max}; the difference in K_m no longer existed 24 hours after such single fighting episodes.

EDITH D. HENLEY
BEATRIZ MOISSET
BRUCE L. WELCH
Friends Medical Science Research Center, Inc., Baltimore, Maryland 21228, and Johns Hopkins University School of Medicine, Baltimore 21205

References and Notes

1. L. L. Iverson, *Advan. Biochem. Psychopharmacol.* **2**, 109 (1970).
2. J. J. Schildkraut and S. S. Kety, *Science* **156**, 21 (1967); S. H. Snyder, *Arch. Gen. Psychiat.* **27**, 169 (1972).
3. A. S. Welch and B. L. Welch, in *The Physiology of Aggression and Defeat*, B. E. Eleftheriou and J. P. Scott, Eds. (Plenum, New York, 1971), pp. 91–142; B. L. Welch and A. S. Welch, in *Aggressive Behavior*, S. Garattini and E. B. Sigg, Eds. (Excerpta Medica, Amsterdam, 1969), pp. 188–202; in *Current Concepts in Amphetamine Abuse*, E. H. Ellinwood and S. Cohen, Eds. (Government Printing Office, Washington, D.C., 1973), pp. 107–115.
4. S. H. Snyder and J. T. Coyle, *J. Pharmacol. Exp. Ther.* **165**, 78 (1969). We used the following modifications of the method of Snyder and Coyle: Krebs-Ringer phosphate medium [W. W. Umbreit, R. H. Burris, J. F. Stauffer, *Manometric Techinques* (Burgess, Minneapolis, 1957), p. 149] was used instead of bicarbonate medium, with room air as the gas phase; 0.01 m*M* pargyline was used to inhibit monoamine oxidase. After homogenates were incubated for 5 minutes in radioactive media and centrifuged, washed pellets were drained and extracted in the same incubation tubes with a nonionic surfactant type of liquid scintillation medium (Instagel, Packard), and tritium was determined in a Packard Tricarb model 3320 refrigerated liquid scintillation spectrophotometer at 35 percent efficiency. The concentration of *dl*-[7-^{3}H]-norepinephrine (as D-bitartrate salt; specific activity, 13.6 or 4.3 c/mmole; New England Nuclear) was held constant in all incubation media, and carrier *dl*-norepinephrine hydrochloride (Calbiochem) dissolved in 1 m*M* hydrochloric acid containing disodium ethylenediaminetetraacetic acid (0.05 mg/ml) was added to vary the concentration of norepinephrine in the media. The concentration of acid vehicle was kept constant at less than 1 percent of the media. The incubation volume was 2 ml, and the amount of tissue homogenate added was equivalent to 5 mg of original cerebral cortex per tube. The uptake of *dl*-[^{3}H]norepinephrine in 5 minutes was determined in triplicate at 37° and 0°C, with and without *d*-amphetamine, at four to eight different concentrations of *dl*-[^{3}H]-norepinephrine from 0.01 to 0.5 μM. The uptake at 0°C was subtracted from that at 37°C and the net uptake was used to determine kinetic constants. Pairs of fighters and appropriate nonfighting controls were killed between 11 a.m. and 2 p.m., and control and experimental tissues were treated identically with respect to time and conditions of incubation, temperature, and centrifugation, thus ensuring a legitimate comparison between paired tissue samples.
5. H. Lineweaver and D. Burk, *J. Amer. Chem. Soc.* **56**, 658 (1934). In all experiments we obtained linear double-reciprocal plots with positive ordinate intercepts, characteristics of a saturable process. The concentration of *d*-amphetamine sulfate was 0.1 μM.
6. Male Swiss albino mice (CD-1, Charles River) were received at 3 weeks of age and housed in groups of eight in opaque plastic cages (23 by 42 by 15 cm) with free access to Purina food and water under controlled conditions of temperature and lighting. They were killed at 3 to 4 months of age.
7. C. O. Rutledge, R. J. Ziance, A. H. Azzaro, *Pharmacologist* **13**, 202 (1971); A. J. Boakes, P. B. Bradley, J. M. Cardy, *Brit. J. Pharmacol.* **45**, 391 (1972).
8. A. S. Welch and B. L. Welch, *Proc. Nat. Acad. Sci. U.S.A.* **60**, 478 (1968); A. M. Goldberg and B. L. Welch, *Science* **178**, 319 (1972).
9. Male CD-1 mice were received at 3 weeks of age and housed in individual opaque plastic cages (15 by 27 by 13 cm). At specified ages they were induced to fight by placing three to ten mice together in a cage for 10 to 15 minutes. During this time they fought intensely, and afterward they were returned to their individual cages.
10. W. Wilbrandt and T. Rosenberg, *Pharmacol. Rev.* **13**, 109 (1961); L. L. Iversen, *The Uptake and Storage of Noradrenaline in Sympathetic Nerves* (Cambridge Univ. Press, Cambridge, England, 1967).
11. M. de V. Cotton, S. Udenfriend, S. Spector, Eds., "New York Heart Association symposium on regulation of catecholamine metabolism in the central nervous system," *Pharmacol. Rev.* **24**, 161 (1972).
12. A. A. Kurland and R. W. Von Korff provided facilities at the Maryland Psychiatric Research Center. L. Braiterman, R. Sanders, and H. Caplan gave technical assistance in portions of this study. D. B. Duncan (Department of Biostatistics, Johns Hopkins University School of Hygiene and Public Health) counseled on statistical analysis. Supported by Friends Medical Science Research Center, Inc., and by National Institute of Mental Health grant MH 18517 to B.L.W. and A. S. Welch.

24 October 1972; revised 2 February 1973

Avalanche Mode of Motion: Implications from Lunar Examples

Abstract. *A large avalanche (21 square kilometers) at the Apollo 17 landing site moved out several kilometers over flat ground beyond its source slope. If not triggered by impacts, then it was as "efficient" as terrestrial avalanches attributed to air-cushion sliding. Evidently lunar avalanches are able to flow despite the lack of lubricating or cushioning fluid.*

An unusual feature at the Apollo 17 landing site has been interpreted as an avalanche deposit (*1, 2*). The Apollo 17 avalanche, as it will be referred to herein, is a thin deposit of bright material that extends 5 km over a dark plain from the base of a mountain massif 2 km high (Fig. 1). This feature may hold important clues to mechanisms of debris transport where air or water are not available as lubricants. If it moved only by gravity, a low effective "friction coefficient" of only 0.2 is implied. This low friction is comparable to that of the Sherman (Alaska), Frank (Alberta), and other terrestrial avalanches in which the long runout has been attributed to air-cushion lubrication (*3, 4*). In this report I compare the Apollo 17 avalanche with similar features on the earth and moon as a means of evaluating transport mechanisms.

The Apollo 17 avalanche covers 21 km^2, 2½ times the area of the Sherman avalanche (*3*). The thickness appears to decrease from perhaps 20 m or more at the mountain base to a few meters at the distal end, as determined from the size of small craters that penetrate the deposit so that their ejecta include darker underlying material (*2*). The thickness averages perhaps 10 m, so that the volume is approximately 200×10^6 m^3. Unlike bright crater rays, the margins of the deposit are fairly distinct against the adjacent dark material.

The thicker, proximal end of the deposit is ridged: low longitudinal ridges are spaced 100 to 200 m apart and are parallel or subparallel to the apparent direction of movement away from the slope. A narrow discontinuous moat several meters deep separates the avalanche deposit from the mountain slope, but it appears to be crossed by the longitudinal ridges. The moat may be analogous to distinctive troughs at some terrestrial rock avalanches (*5*).

A striking feature of the avalanche is that it appears to have hardly been influenced by preexisting topographic irregularities. An older crater 1 km in diameter and 60 m deep near the center of the deposit is clearly visible and apparently evenly mantled, as is also a fresh-appearing wrinkle-like ridge (Fig. 1).

The source of the avalanche was probably fine-grained regolith on the adjacent mountain slope (most of this slope is covered by such regolith). Two small isolated blocky areas of possible outcrop occur high on the slope above the avalanche, but, unlike smaller avalanches (see below), there is no obvious scar or rock ledge.

This avalanche is the largest example of its type yet recognized on the moon (*6*) and may therefore be anomalous. Smaller avalanche deposits have been recognized on the walls of several craters 10 to 30 km in diameter (Fig. 2, A to C). A rare few extend beyond the steep crater wall out onto the floor of the crater (Fig. 2, A and B).

These crater-wall deposits show distinct margins which suggest that the material moved as flows. Blocks are not visible in the deposits at the resolution of the photographs (~ 3 m). Characteristically the source can be identified at the top of the crater as an outcropping ledge or bright horizontal stripe suggestive of an outcrop. The avalanches are clearly due to local slope failures.

The lack of an easily identified source ledge for the Apollo 17 avalanche and its unusually large size suggest that its origin might differ from those in the craters. One possibility is that it is associated with a ray of impact debris.

Similar avalanches have, in fact, been triggered by secondary impacts. Figure 2D shows diffuse bright rays from a very fresh crater. In two areas near the primary crater (Fig. 2, E and F) the rays impinge on old crater walls that slope away from the primary crater; the rays extend from the slopes out onto flats (the old crater floors) in lobate avalanche-like forms with distinct frontal margins. Small elongate grooves and herringbone patterns that are characteristic of secondary impact craters are present on the slopes at the proximal end of each lobe. Like the Apollo 17 avalanche, the bright debris in these lobes is finer grained than the resolution limit of about 3 m and is very thin; preexisting craters are evenly coated and clearly visible, and the largest lobes have faint longitudinal ridging on the base of the slope. These ray lobes evidently formed as a result of the impact of ejecta on a regolith-covered slope, which triggered avalanches that moved out across the flat beneath the slope as fragmental flows with definite margins. Elsewhere the crater ejecta simply splashed (*r* in Fig. 2, E and F).

For the Apollo 17 avalanche there are no recognizable secondary-impact or herringbone patterns and no clearly associated rays. However, the direction of movement of the avalanche coincides with the orientation of a ray in Mare Serenitatis from the crater Tycho, and an origin by the splash of ejecta from a distant crater such as Tycho, or even by primary impact such as by a cluster of cometary debris, cannot be discounted. If, however, evidence obtained from the Apollo 17 mission points to a local slope failure rather than a ray origin, the Apollo 17 avalanche has broad implications concerning mechanisms of avalanche transport. One may demonstrate this by comparing this avalanche with terrestrial avalanches.

A number of large rock avalanches on the earth also extend well beyond the base of the steep slopes from which they originated. These avalanches traveled at high velocity (commonly 40 m/sec or more), and many moved out so far beyond the base of the slope that a surprisingly low effective "friction coefficient" is indicated. The low friction has been attributed to fluidization of the particles caused by mixing with air (*7*) or to sliding on a cushion of trapped air (*3, 4, 8*).

As a rule, large rock avalanches and those that fall from great height move out farther beyond the base of the slope and have lower apparent coefficients of friction. This is illustrated in Fig. 3, where potential energy is plotted against

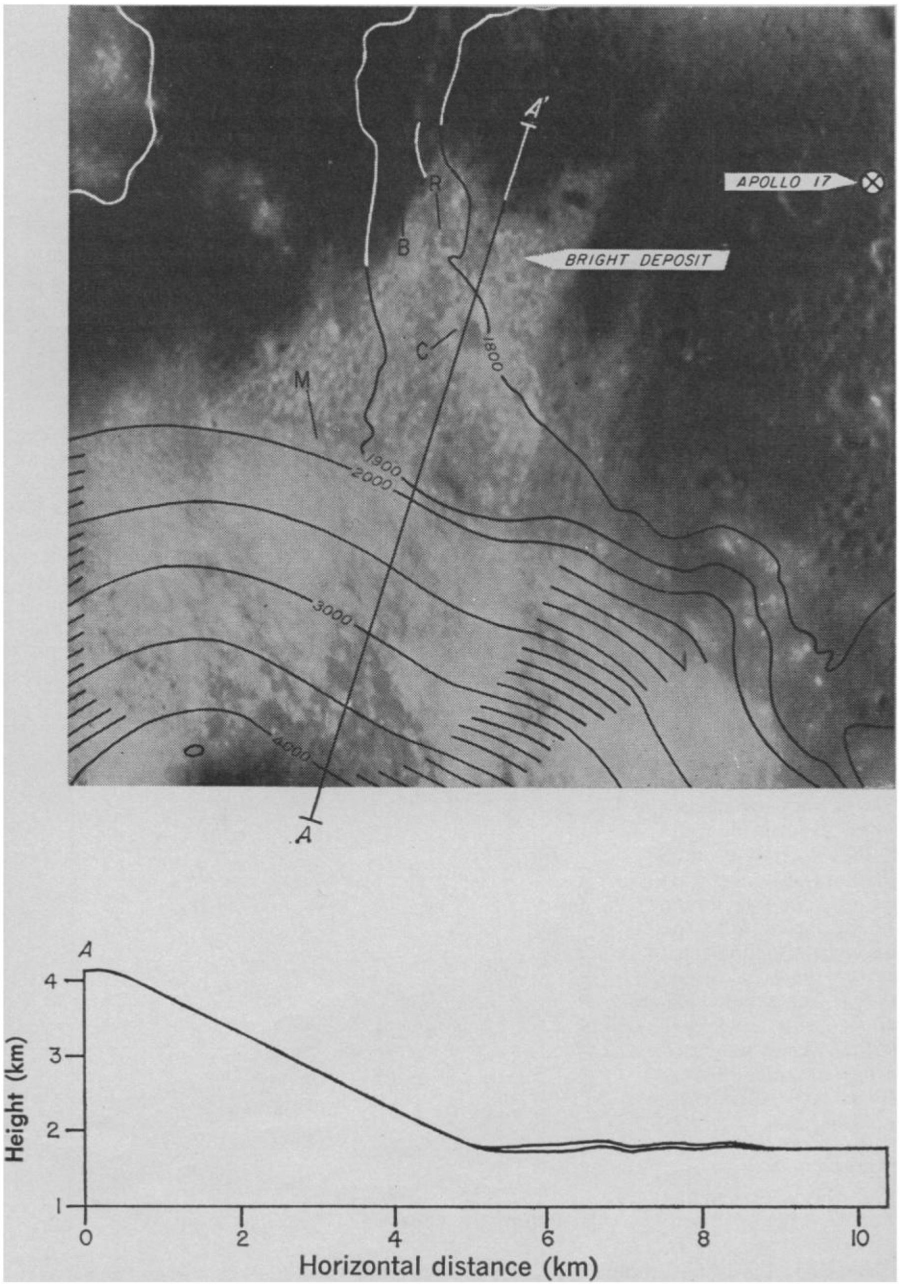

Fig. 1. Apollo 15 photo of the Apollo 17 landing site. The bright deposit overlies a dark plain and appears to be an avalanche from the massif to the south. Contours are in meters; *A–A'*, line of profile shown; *C*, buried crater; *R*, ridge; *B*, bright margin; and *M*, moat.

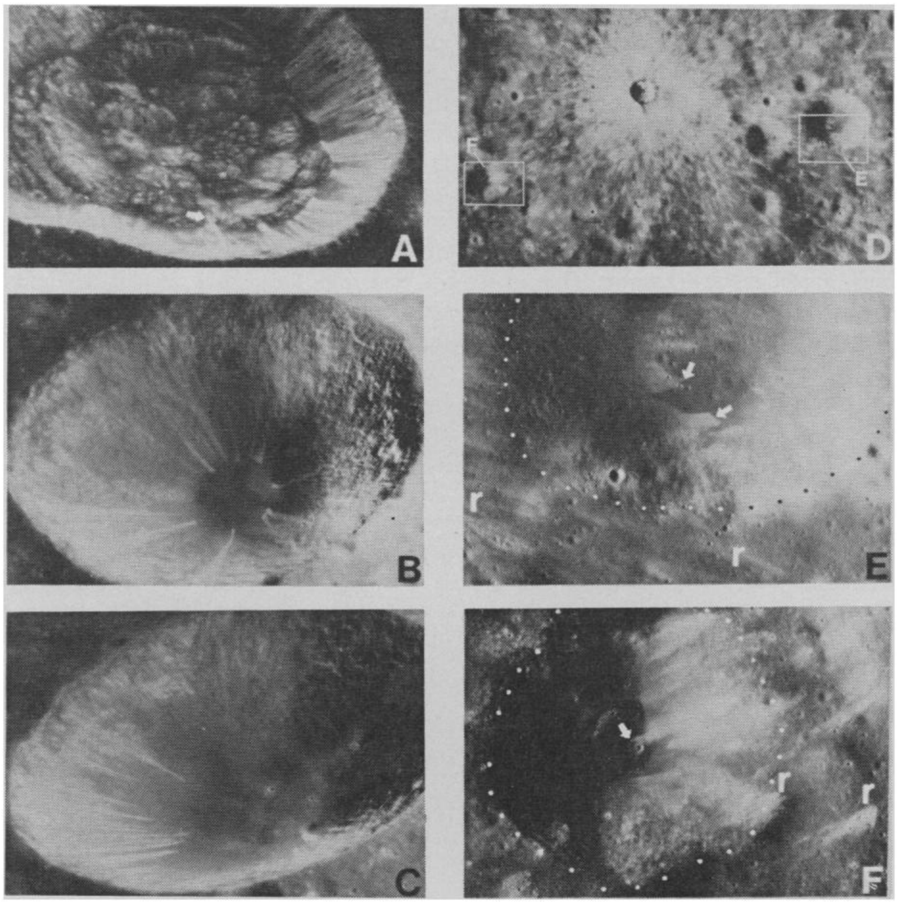

Fig. 2. Avalanche deposits on the walls of lunar craters. (A) Jansen B crater (17 km in diameter). The arrow shows the most prominent avalanche, which appears to cross out onto the crater floor [NASA photo AS15 panoramic 9871]. (B) Lalande A crater (12 km in diameter) [NASA photo AS16 panoramic 5400]. (C) Isidorus D crater (15 km in diameter) [NASA photo AS16 panoramic 4502]. (D) Bright rays around a crater 3 km in diameter near Gagarin. The rays are diffuse streaks except in the two areas shown in (E) and (F) [NASA photo AS16 metric 0102]. (E) Detail of the ray pattern. Inside an old crater (rim crest dotted) two rays impinged on a slope facing away from the primary crater, apparently initiating avalanche lobes (arrows). Elsewhere the rays are diffuse smears (*r*) [NASA photo AS16 panoramic 8934]. (F) Detail of a similar ray-initiated avalanche on the other side of the primary crater [NASA photo AS16 panoramic 8941].

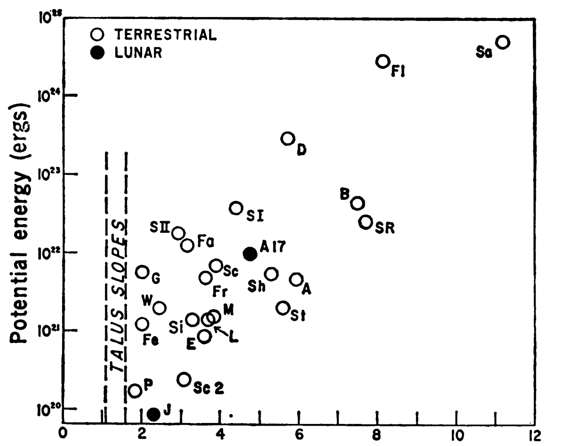

Fig. 3. Potential energy of large rock avalanches, plotted against the ratio of the maximum total horizontal distance traveled to the maximum total height of fall. The data are approximate but clearly show a trend toward increased efficiency with increased energy. Terrestrial avalanches are identified as follows: *A*, Allen (*14*), *B*, Blackhawk (*4*); *D*, D'Ousoi (*15*); *E*, Elm (*4*); *Fa*, Fairweather (*14*); *Fe*, Fernandina (*16*); *Fl*, Flims (*5*, *15*); *Fr*, Frank (*4*, *5*); *G*, Goldau (*5*); *L*, Little Tahoma Peak 3 (*8*); *M*, Madison (*17*); *P*, Puget Peak (*18*); *Sa*, Saidmerreh (*15*); *S I*, Sawtooth Ridge I (*5*); *S II*, Sawtooth Ridge II (*5*); *Sc*, Schwan 1 (*14*); *Sc 2*, Schwan 2 (*14*); *Sh*, Sherman (*3*); *SR*, Silver Reef (*4*); *Si*, Sioux (*14*); *St*, Steller (*14*); *W*, Wolf (*16*). Lunar avalanches are: *A17*, Apollo 17; and *J*, Jansen B crater.

the ratio of the maximum horizontal distance to the maximum vertical drop. The potential energy is calculated in terms of the estimated weight multiplied by the average height of fall. The ratio of the horizontal to the vertical distance traveled represents a measure of the "efficiency" of movement, and for sliding avalanches this ratio may be thought of as the inverse of the friction coefficient. Ratios larger than 1.4 to 1.7, which correspond to the common angle of repose of rockfall talus (30° to 35°), generally indicate movement beyond the base of the originating slope. Figure 3 suggests that avalanches with energies of less than about 10^{20} ergs do not move far beyond their slopes. More energetic avalanches are more efficient.

For comparison, let us assume that the Apollo 17 avalanche fell from near the top of the mountain. Its potential energy was then 10^{22} ergs, and the ratio of the maximum horizontal distance traveled to the maximum fall is about 4.7 (*9*). This would correspond to a friction coefficient of 0.2. Plotted on Fig. 3, these data for the Apollo 17 avalanche (A17) fall well within the range of values for terrestrial avalanches. If the thickness of the deposit averages less than 10 m, or, if the source was lower on the slope, the Apollo 17 feature would plot lower and more to the right, corresponding to an even greater efficiency.

The Sherman (Sh) and Frank (Fr) avalanches, both of which have been attributed to air-cushion sliding (*4*), plot nearby. The Apollo 17 avalanche appears to have been comparably efficient, yet with no air available for cushioning or lubrication. The efficiency of the smaller lunar avalanche in Fig. 2A is also comparable with that of terrestrial examples near the lower energy threshold for efficient movement (*J* in Fig. 3).

If no fluid phase is available for lubricating or fluidizing lunar avalanches, how did they move? The lack of a lubricant makes it unlikely that they slid; more likely they flowed. Rock avalanches at Little Tahoma Peak (Washington) (*8*) and Bandai San (Japan) (*10*) were described as behaving like fluids of rapidly moving rock fragments. Small inefficient flows of dry rock fragments also occur in sand runs and allied flows of loess and silt (*11*), and are a familiar experience to persons hiking on loose scree. Although air buoyancy is a factor on the earth, the fluidity of these examples probably involves primarily interactions between the particles (*12*). The lunar avalanches suggest that, irrespective of air buoyancy, avalanches can behave efficiently like fluids composed of rapidly moving particles.

The idea that masses of rock fragments can exhibit fluid behavior in the absence of liquids or gases has important implications for geologic transport mechanisms on the moon. For instance, base surges (*13*) or analogous radial flows could be produced by impact events in the absence of a gas phase. Furthermore, where geologic characteristics such as relict stratigraphy do not demand it, it may not be necessary to posit air lubrication to account for efficient avalanches on the earth.

Data from the Apollo 17 mission may make it possible to determine whether the large avalanche at the landing site originated locally and moved in the absence of gas. In any event, the characteristics of smaller lunar avalanches (Fig. 2) strongly imply that gas-free rock flows occur.

Note added in proof: Rocks collected from the Apollo 17 bright mantle are like those from the adjacent mountain to the south, which supports the avalanche interpretation (*19*). Photographic evidence obtained during the Apollo 17 mission increases the likelihood that this avalanche was triggered by secondary impacts from Tycho (*19*). The small sizes of secondary craters in the vicinity suggests that the kinetic energy added to the avalanche by these impacts is small compared to the potential energy of falling (10^{22} ergs). The plotted position of the Apollo 17 avalanche in Fig. 3, therefore, would change but little if this kinetic energy were added; the problem of the "efficiency" of this avalanche remains.

KEITH A. HOWARD
U.S. Geological Survey,
Menlo Park, California 94025

References and Notes

1. D. H. Scott, B. K. Lucchitta, M. H. Carr, "Geologic maps of the Taurus-Littrow region of the moon—Apollo 17 premission maps" [*U.S. Geol. Surv. Misc. Geol. Invest. Map I-800* (1972)].
2. E. W. Wolfe, V. L. Freeman, W. R. Muehlberger, J. W. Head, H. H. Schmitt, J. R. Sevier, *Geotimes* **17** (No. 11), 14 (1972).
3. R. L. Shreve, *Science* **154**, 1639 (1966).
4. ———, *Geol. Soc. Amer. Spec. Pap. 108* (1968).
5. M. R. Mudge, *Geol. Soc. Amer. Bull.* **76**, 1003 (1965).
6. Another type of apparent lunar debris flow is represented by a much larger and thicker lobate avalanche which extends radially outward from the crater Tsiolkovsky. This lobe may have been mobilized by impact fluids, and its radial orientation suggests that the driving force included the cratering event as well as gravity.
7. P. E. Kent, *J. Geol.* **74**, 79 (1966); R. L. Shreve, *Geol. Soc Amer. Bull.* **79**, 653 (1968). Dry snow avalanches behave as density currents of mixed air and particles [M. Mellor, *U.S. Army Cold Regions Res. Eng. Lab. Monogr.* (part 3, sect. A3) (1968), p. 17], and the fluid behavior of some rock avalanches has been similarly attributed [see (*8, 11*)].
8. D. R. Crandell and R. K. Fahnestock, *U.S. Geol. Surv. Bull. 1221-A* (1965).
9. This assumes a specific gravity of 2 (so that the weight of the deposit on the moon is 6.5×10^{16} dynes), an average height of fall of 1700 m, and distances of 1900 m (vertical) and 9000 m (horizontal) from the top of the denuded zone to the distal end.
10. S. Sekiya and Y. Kikuchi, *J. Coll. Sci. Imp. Univ. Tokyo* **3** (part 2), 91 (1889).
11. D. J. Varnes, *Nat. Res. Counc. Highw. Res. Board Spec. Rep. 29* (1958), p. 20.
12. R. A. Bagnold [*Proc. Roy. Soc. Ser. A Math. Phys. Sci.* **225**, 49 (1954)] suggests a theoretical approach for particle flow in which inertial effects dominate over fluid-viscosity effects.
13. G. A. Young, *The Physics of the Base Surge* (U.S. Naval Ordnance Laboratory, White Oak, Md., 1965).
14. A. S. Post, *Nat. Acad. Sci. Publ. 1603* (1968), p. 266; *U.S. Geol. Surv. Prof. Pap. 544-D* (1967). I have assumed average thicknesses of 3 m for the Allen, Fairweather, and Schwan 1 avalanches, 5 m for the Schwan 2 avalanche, 2 m for the Sioux avalanche, and 1.3 m for the Steller avalanche.
15. J. V. Harrison and N. L. Falcon, *J. Geol.* **45**, 296 (1938).
16. K. Howard, unpublished data, Galápagos Islands.
17. J. B. Hadley, *U.S. Geol. Surv. Prof. Pap. 435-K* (1964), p. 107.
18. M. C. Hoyer, *Geol. Soc. Amer. Bull.* **82**, 1267 (1971).
19. W. R. Muehlberger *et al.*, in *Apollo 17 Preliminary Science Report* (National Aeronautics and Space Administration, Washington, D.C., in press).
20. I thank G. Plafker, E. W. Wolfe, and H. H. Schmitt for discussions and helpful suggestions. Supported by NASA contract W13,130 and experiment S-222. Publication authorized by the director, U.S. Geological Survey.

7 December 1972; revised 9 February 1973

Monoclinic Hydroxyapatite

Abstract. *The existence of a monoclinic phase of hydroxyapatite, $Ca_5(PO_4)_3OH$, has been confirmed, by single-crystal structure analysis (weighted "reliability" factor = 3.9 percent on $|F|^2$). The structure has space group* $P2_1/b$, a = *9.4214(8) angstroms,* b = 2a, c = *6.8814(7) angstroms, and* $\gamma = 120°$, *and is analogous to that of chlorapatite. The distortions from the hexagonal structure with which the monoclinic structure is pseudosymmetric are similar to those in chlorapatite, including enlargement of that triangular array of oxygen atoms in which the chlorine ion or, in hydroxyapatite, the hydroxyl hydrogen ion is approximately centered. The hydroxyapatite specimen was prepared by the conversion of a single crystal of chlorapatite in steam at 1200°C, was mimetically twinned, and was approximately 37 percent monoclinic.*

The agriculturally and scientifically important apatite minerals, their technologically (lighting, catalysis, laser host) important synthetic counterparts, and the closely related "mineral" portion of bones and teeth have, until recently, been thought to occur only with hexagonal crystal symmetry in crystallographic space group $P6_3/m$. A monoclinic pseudohexagonal form, space group $P2_1/b$, of both synthetic (*1, 2*) and mineral (*3*) forms of chlorapatite has recently been reported for specimens with nearly stoichiometric (for example, less than 5 to 15 percent deficient) chlorine contents. In both forms the chlorine ions occur in columns. In the monoclinic form they are fully ordered within columns and the columns are ordered relative to each other (*1, 4*). In the hexagonal form the lack of full intracolumn ordering is statistically representable as twofold disorder of the chlorine positions about mirror planes which, in the monoclinic form, become glide planes.

In hexagonal hydroxyapatite the hydroxyl ions are similarly arranged in columns in twofold disorder with the O→H direction pointing away from the mirror planes passing through the nearest coordinating calcium ions (*5*). It was recognized (*5*) that adjacent hydroxyl ions in a given column must occur in a head-to-tail fashion, that is, O–H O–H O–H, otherwise the H–H approach would be too close. It was later shown (*6*) that the fluorine impurities in the mineral (from Holly Springs, Georgia) were distributed and that they provided reversal points for the sense of the O–H direction within a column. It was then conjectured [see, for example, Young (*7*) and Elliott (*8*)] that a hydroxyapatite specimen, sufficiently free of impurities and vacanies so that no significant number of such reversal points were present within the column, might also exhibit intercolumn ordering and, hence, the monoclinic $P2_1/b$ space group, analogously to chlorapatite. Elliott reported (*9*) that the diffraction pattern of hydroxyapatite crystals prepared from essentially stoichiometric chlorapatite single crystals, heated in steam at 1200°C for 2 weeks (*10*), exhibited "extra" reflections explicable on the basis of